EasyChair Preprint

№ 3438

Comparison of Thermodynamic Performances Between Room Cooling and Forced-Air Cooling: Evaluation by Produce Temperature and Effects of Measurement Positions

Guan-Bang Wang and Xin-Rong Zhang

May 18, 2020

Comparison of thermodynamic performances between room cooling and forced-air cooling: evaluation by produce temperature and effects of measurement positions

Guan-Bang Wang[a], Xin-Rong Zhang[b]

[a] Department of Energy and Resources Engineering, College of Engineering, Peking University, Beijing, China, coewgb@pku.edu.cn

[b] Department of Energy and Resources Engineering, College of Engineering, Peking University, Beijing, China, xrzhang@pku.edu.cn, ***CA***

Abstract:

Room cooling (RC) and forced-air cooling (FAC) are traditional precooling methods for postharvest horticultural products. The performances of these methods were widely investigated in terms of cooling time, energy consumption and related airflow and heat transfer characteristics. The authors recently proposed a thermodynamic model to evaluate the performances based on the experimental measurement of the produce temperature regarding the convective heat transfer between the air and products and related airflow strategies resulting in significant irreversible loss. Because of the temperature varying within a single bin and even within an individual produce, the performances indicated from this thermodynamic model are affected by the sampling positions of the produce temperature. In this study, based on the experiments with 30 bins of postharvest apples, such effects are respectively considered for the estimations of the volumetric mean temperature of an individual produce and the different temperature measurement positions within a single bin. The thermodynamic performances considering such effects are compared between RC and FAC. The results indicate that different temperature measurement positions result in higher differences of above 20-30% for the COPs and entropy generation ratio than that for other thermodynamic performances, while different methods to estimate the volumetric mean produce temperature generally resulted in limited effects on the thermodynamic performances.

Keywords:

Comparative Study, Postharvest Precooling, Temperature Measurement, Thermodynamic Performance.

1. Introduction

Precooling is a typical postharvest operation to quickly remove the field heat from the produce and lower the produce temperature [1]. Room cooling (RC) and forced-air cooling (FAC) are typically adopted for commercial precooling applications because they are simple, cost-effective and compatible with a wide range of produce especially for fruits. The produce for RC is placed inside a cold room and subjected to convective heat transfer with the cold air at the package surface under the ventilation conditions therein [2]. FAC enables the cold air to flow through the packaging system of the produce under the pressure difference across it generated by the ventilation devices and the heat convection between the cold air and the produce is achieved inside the package [3]. Consequently, the process of RC tends to be slower and more heterogeneous when compared with that of FAC and requires better ventilated packaging system. On the contrary, the large airflow resistance inside the produce package leads to the use of high-power centrifugal fans for FAC and thus large amount of electricity consumption. It was estimated that the total electricity consumption for FAC could be as high as around 60 kWh per metric ton of produce, while 28% was contributed by the ventilation fans which was the second highest just behind the fruit cooling with 36% contribution [4]. Therefore, both of RC and FAC have their own advantages and disadvantages, and the performances should be compared between them.

The energy usage is always of interest regarding to the performances of the precooling process and the refrigeration system. Mukama et al. [5] conducted comprehensive energy accounting for FAC

and found that a significant part of the electricity consumption as well as the cooling load was contributed by the fans. In other words, large part of the refrigeration capacity is used to remove the heat generated by the fans rather than the produce. Hence, the efficiency of FAC process, especially for the convective heat transfer driven by such fans, should be revisited and compared with that of RC process. Thermodynamic parameters are suitable for evaluation of such processes. The optimization of the convective heat transfer was extensively investigated by the minimization of entropy [6] and exergy [7, 8] and the extremum of entransy [9, 10]. In fact, exergetic parameters were introduced into the process analyses of food nutrition and production [11] and food industry [12]. For example, Ozturk and Hepbasli [13] conducted exergy analysis of a vacuum cooling system through experimental measurement. For air-based precooling processes, Wang and Zhang [14] recently established a multiscale model of the air-based precooling processes to perform comprehensive thermodynamic analyses using different parameters based on the experimental measurement of produce temperature.

The aforementioned performance evaluation must be based on the time-temperature history of produce [15]. The produce temperature could be obtained from the numerical simulation for RC [16] and FAC [17], but the results had to be validated by the corresponding experiments. There was uncertainty of temperature measurement at different positions within the produce individuals [18]. The temperature distribution inside the single produce could be estimated either by the simple heat transfer model [19] or the one-dimensional numerical model [20]. Jedermann et al. [21] further indicated the spatial variations of temperature inside a single pallet and the refrigerated space. The corners of the pallet were identified as the best positions for temperature measurement [22] and the temperature distribution inside a pallet could be predicted by neural network models based on the measured temperature at these positions [23]. A simplified heat transfer model was also established for RC to predict the produce temperature at different positions inside the cold room [24] according to the experimental measurements of the characteristics of airflow and heat transfer [25]. The distribution of the produce temperature during the commercial FAC was correlated for the temperature prediction at different positions [26].

The aforementioned literature showed the heterogeneous temperature distribution and the uncertainty of the measured temperature with limited sampling positions from the single produce individual to the full-scale commercial applications of precooling processes. The heterogeneity and uncertainty will then affect the evaluation of overall process performances such as the thermodynamic indicators based on the measured temperature. Consequently, in the present study, the measurement of the produce temperature is achieved with a high resolution to investigate the aforementioned effects of measurement positions on the thermodynamic performances evaluated by the measured produce temperature during the experiments for RC and FAC. On one hand, both of the core temperature and surface temperature are measured for the sampled produce individuals and the estimation of the produce temperature is compared among different heat transfer models. On the other hand, the temperature measurement is conducted in each bin and the sampling positions change from the center to the corners with different rounds of experiments so that the effects of different measurement positions in a single bin on the thermodynamic performances can be obtained. The experimental setup and the thermodynamic model for performance evaluation by measured produce temperature are respectively shown in sections 2 and 3. The effects of the temperature measurement positions within a produce individual and a single bin are then discussed in section 4. The concluding remarks are finally given in section 5.

2. Experimental setup

2.1. Precooling processes and system configuration

During the precooling processes, the produce temperature reduces from the initial value of 21.0°C to the target value of 2.5°C. Three replicated experiments are conducted for different sampling positions of produce temperature during RC and FAC. The experiments of RC and FAC are

conducted alternatively, so the system layout is rearranged for each round of experiment, which can be then considered to be independent from others.

All the experiments are conducted in a cold room with the dimension of 4.0 m × 3.4 m × 2.8 m which is built indoors. As shown in Fig. 1, three axial fans with the diameter of 0.3 m and the rated power of 210 W in total are used for a ceiling suspended cooling unit (Panasonic CC-CV9000H, Osaka, Japan). The cooling unit is installed on one side of the room with a distance of 0.4 m from the room wall. The combined unit of compressor and condenser (Emerson ZXD050E-TFD, St. Louis, USA) is also installed indoors just outside the cold room.

The system configuration of RC is given in Fig. 1(a). 3 bins are stacked on each pallet, and 10 pallets are symmetrically arranged in two lines respectively on the east and west of the cold room with the distance of 0.2 m between each two pallets. The cold air ejected from the cooling unit flows above in the cold room and falls after reaching the room wall. The cold air then passes by the produce stacks and goes back to the cooling unit.

As shown in Fig. 1(b), the stacks of bins are closely placed in two lines without changing the relative position of each bin for FAC. A distance of 0.2 m between the two lines of bins is used for the air corridor, one end of which is connected to an air duct and subsequently a centrifugal fan (Tafeng HA1100, Zhejiang, China) with the rated power of 1.1 kW and the air flow rate of 2200 m^3/h. The top and end surfaces of the stacks as well as the top and the other end of the air corridor are covered with the tarp. Consequently, the cold air flows through the produce stacks from the outer side of the bins to the air corridor and then is exhausted by the centrifugal fan through the air duct.

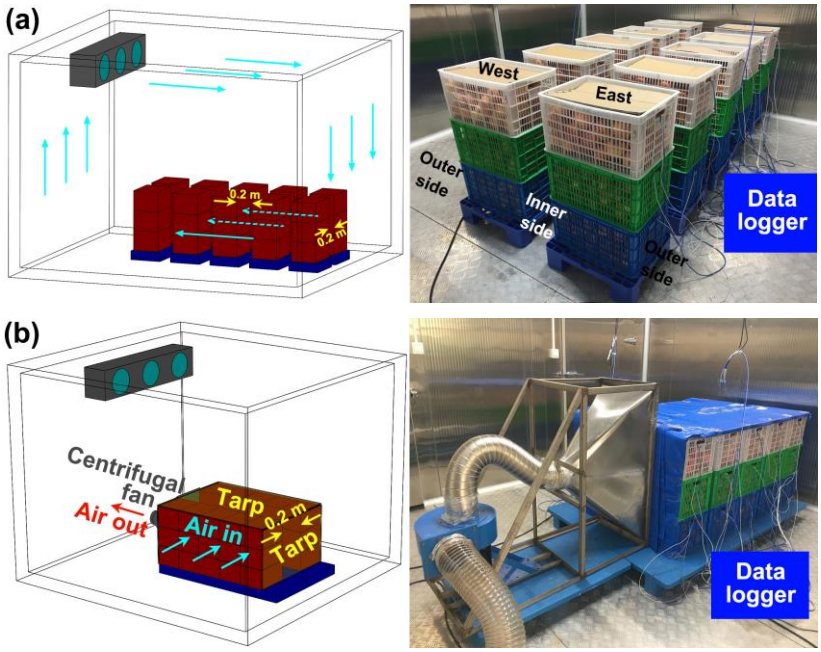

Fig. 1. System configurations of RC and FAC.

2.2. Apple fruit and packaging system

'Fuji' apples (Malus domestica Borkh, cv. Fuji) are harvested at a nearby orchard in Beijing in September, 2019. The apples without visual defects and abnormal shapes are placed in 30 reusable high-density polyethylene (HDPE) plastic bins. The plastic bin is 0.48 m × 0.35 m × 0.27 m with 40% ventilation slots on the surfaces. The cardboard is placed at the bottom of each bin and at the top of bins at the top layers. Each bin with the apples is weighted on average to be 15.24 kg with the standard deviation of 0.09 kg. An apple is sampled in each bin for further measurement. The mean mass and diameter of the sampled apples are 217.25 g and 72.89 mm with the standard deviations of 35.37 g and 4.69 mm respectively.

2.3. Measurement of produce temperature

Both of the surface and core temperatures of the sampled apple are measured, while the sampled apple is placed at different positions inside the bin as shown in Fig. 2 at different rounds of experiments. The positions are symmetrically arranged for the bins on the west and east respectively represented by "+" and "×" so that more positions can be included in the analyses as the system configuration is also symmetrical. At the same round of experiment, the sampling positions are in the center, at the outer side and top layer on the west and bottom layer on the east or at the inner side and bottom layer on the west and top layer on the east. Platinum resistance thermometers (Heraeus PT100, Hanau, Germany) with the accuracy of ± 0.15°C and the applicable range of -60°C to 220°C are used for the temperature measurement. The measured temperature is programmed to be collected in every one minute by connecting the temperature sensors to the data-logger.

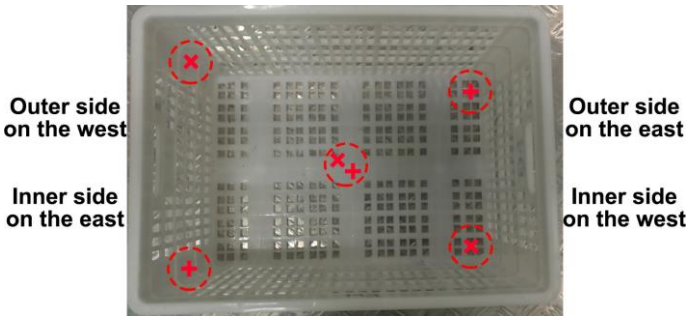

Fig. 2. Sampling positions of produce temperature in each bin. "×" represented the positions for the bins on the west, while "+" represented the positions for the bins on the east.

The volumetric mean temperature of the sampled apple is calculated according to the measured core and surface temperatures for further thermodynamic analyses. The heat transfer inside an apple can be considered to be one-dimensional unsteady heat conduction inside a sphere with internal heat generation as formulated in Eq. (1).

$$\begin{cases} \frac{\partial^2 T}{\partial r^2} + \frac{2}{r}\frac{\partial T}{\partial r} + \frac{\dot{q}}{\lambda} = \frac{\rho C}{\lambda}\frac{\partial T}{\partial t}, 0 < r < R, t > 0 \\ T = T_c(t), r = 0, t > 0 \\ T = T_s(t), r = R, t > 0 \\ T = T_o, 0 \le r \le R, t = 0 \end{cases} \quad (1)$$

where t is the time, T is the temperature, r is the radial coordinate, R is the radius, λ is the thermal conductivity, ρ is the density, C is the specific heat, $\dot{q}$ is the volumetric heat generation rate and the subscripts c, s, o respectively represent the core, surface and initial state. The volumetric heat generation rate is calculated for respiration heat as given in Eq. (2) [27].

$$\dot{q} = \rho \dot{Q}_{res} = \frac{898 \times 10.7 \times 5.6871 \times 10^{-4}}{3600} \left[\frac{9}{5} \times (T - 273.15) + 32\right]^{2.5977} \quad (2)$$

where $\dot{Q}_{res}$ is the rate of respiration heat generation per unit mass. The temperature distribution inside the sampled apple can be then obtained by solving Eq. (1) with the measured core and surface temperatures as the boundary conditions. The volumetric mean temperature can be further calculated as given in Eq. (3).

$$T_m = \frac{3}{4\pi R^3} \int_0^R T(r) 4\pi r^2 \mathrm{d}r \quad (3)$$

where the subscript m represents the mean value. The volumetric mean temperature of the sampled apple can be also calculated as shown in Eq. (4) based on the simple heat transfer model [19].

$$T_m = T_c + (T_s - T_c)\left(\frac{3}{4}\right)^2 \quad (4)$$

3. Thermodynamic model

Produce cooling is the ultimate objective of the postharvest precooling processes. Consequently, the authors previously proposed a multiscale thermodynamic system shown in Fig. 3 to evaluate the thermodynamic performances based on the measured produce temperature [14]. In other words, the process performances of energy, entropy, exergy and entransy are derived and evaluated according to the following thermodynamic analysis using the volumetric mean temperature of the sampled apple and other experimental parameters given in Table 1.

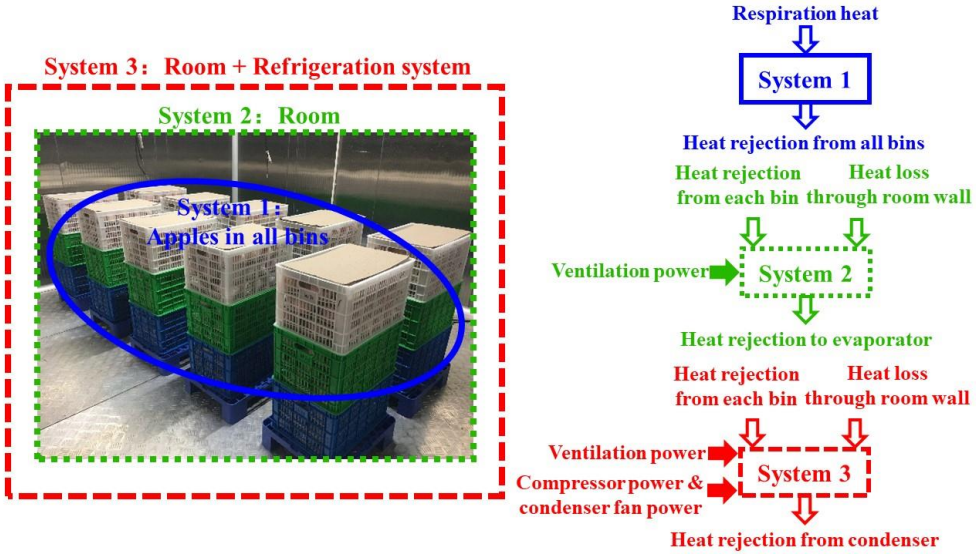

Fig. 3. Schematic illustration of multiscale thermodynamic system for RC and FAC.

Table 1. Constant experimental parameters.

Parameter		Value (Unit)
Apple thermal conductivity		0.463 (W/m·K) [28]
Apple density		898 (kg/m^3) [28]
Apple specific heat		3829 (J/kg·K) [28]
Time step		60 (s)
Reference temperature		263.15 (K)
Evaporation temperature		274.15 (K)
Condensation temperature		312.15 (K)
Initial produce temperature		294.15 (K)
Target produce temperature		275.65 (K)
Overall heat transfer coefficient	Side wall	0.014 (W/m^2·K) [29]
	Ceiling and floor	0.010 (W/m^2·K) [29]
	Door	0.032 (W/m^2·K) [29]
Surface area	Side wall	39.92 (m^2)
	Ceiling and floor	13.60 (m^2)
	Door	1.52 (m^2)

3.1. Bin scale (system 1)

System 1 is the apples inside all bins where the heat input is the respiration heat generated by apples and the heat output is the heat rejection from all bins. The volumetric mean temperature of the sampled apple is used to represent that for each apple within the same bin. The energy balance of system 1 is given in Eq. (5).

$$\frac{M_i\left(h_i^{(n)}-h_i^{(n-1)}\right)}{\Delta t}=\frac{M_i C_i\left(T_{m,i}^{(n)}-T_{m,i}^{(n-1)}\right)}{\Delta t}=M_i\frac{\dot{Q}_{res,i}^{(n)}+\dot{Q}_{res,i}^{(n-1)}}{2}-\dot{Q}_{cool,i}^{(n)} \quad (5)$$

where M is the total mass of apples in the same bin, h is the specific enthalpy, Δt is the time step, $\dot{Q}_{cool}$ is the heat rejection rate from the bin, the subscript i represents the ith bin and the superscript (n) represents the nth time step. The sum of the heat rejection from all bins is subsequently used for the evaluation of the thermodynamic performances at larger scales.

3.2. Room scale (system 2)

System 2 is composed of the room wall and room space excluding the apples. The heat rejection from all bins, the heat loss to the room space through the room wall as well as the ventilation power are included in the input, while heat rejection to the evaporator is the only output. The heat loss rate can be calculated as given in Eq. (6).

$$\dot{Q}_{loss}^{(n)}=\sum_j K_j A_j\left(T_{or}-\frac{T_{ir}^{(n)}+T_{ir}^{(n-1)}}{2}\right) \quad (6)$$

where the subscript j represents the jth part of the room wall, K is the overall heat transfer coefficient and A is the surface area. The temperature inside the cold room represented by the subscript ir is monitored and controlled at around 2.5°C with small fluctuations due to the on-off strategy of the refrigeration system. Since the cold room is built indoors, the outside temperature represented by the subscript or keeps at 21.0°C because of the building insulation. The energy balance of system 2 is given in Eq. (7).

$$\sum_i \dot{Q}_{cool,i}^{(n)}+\dot{Q}_{loss}^{(n)}+\dot{W}_{ven}-\dot{Q}_{eva}^{(n)}=0 \quad (7)$$

where $\dot{Q}_{eva}$ is the heat rejection rate to the evaporator and $\dot{W}_{ven}$ is the ventilation power which is respectively 210 W and 1310 W for RC and FAC. The entropy balance of system 2 is given in Eq. (8).

$$\sum_i \frac{2\dot{Q}_{cool,i}^{(n)}}{T_{s,i}^{(n)}+T_{s,i}^{(n-1)}}+\frac{\dot{Q}_{loss}^{(n)}}{T_{or}}-\frac{2\dot{Q}_{eva}^{(n)}}{T_{ir}^{(n)}+T_{ir}^{(n-1)}}+\dot{S}_{gen,in}^{(n)}=0 \quad (8)$$

where $\dot{S}_{gen,in}$ is the entropy generation rate within system 2. The exergy balance of system 2 is given in Eq. (9).

$$\sum_i \dot{Q}_{cool,i}^{(n)}\left(1-\frac{2T_0}{T_{s,i}^{(n)}+T_{s,i}^{(n-1)}}\right)+\dot{Q}_{loss}^{(n)}\left(1-\frac{T_0}{T_{or}}\right)-\dot{Q}_{eva}^{(n)}\left(1-\frac{2T_0}{T_{ir}^{(n)}+T_{ir}^{(n-1)}}\right)+\dot{W}_{ven}-\dot{E}x_{D,in}^{(n)}=0 \quad (9)$$

where $\dot{E}x_{D,in}$ is the exergy destruction rate within system 2. The entransy balance of system 2 is given in Eq. (10).

$$\sum_i \dot{Q}_{cool,i}^{(n)}\left(\frac{T_{s,i}^{(n)}+T_{s,i}^{(n-1)}}{2}\right)+\dot{Q}_{loss}^{(n)}T_{or}+\left(\dot{W}_{ven}-\dot{Q}_{eva}^{(n)}\right)\frac{T_{ir}^{(n)}+T_{ir}^{(n-1)}}{2}-\dot{\Phi}_{in}^{(n)}=0 \quad (10)$$

where $\dot{\Phi}_{in}$ is the entransy dissipation rate within system 2.

3.3. Ensemble scale (system 3)

The addition of the refrigeration system to system 2 results in system 3 which is identified as the ensemble scale. In comparison with system 2, the additional work input of compressor and condenser fan power is required and the heat output changes into the heat rejection from the condenser. The energy balance of system 3 is given in Eq. (11).

$$\sum_i \dot{Q}_{cool,i}^{(n)}+\dot{Q}_{loss}^{(n)}+\dot{W}_{ven}+\dot{W}_{com\&con}^{(n)}-\dot{Q}_{con}^{(n)}=0 \quad (11)$$

where $\dot{Q}_{con}$ is the heat rejection rate from the condenser and $\dot{W}_{com\&con}$ is the sum of compressor power and condenser fan power. The on-off strategy of the refrigeration system leads to discontinuous requirement of compressor and condenser fan power [30]. Hence, power input to the

combined unit of compressor and condenser is not measured but estimated by the heat rejection rate to the evaporator $\dot{Q}_{eva}$ and the COP of the refrigeration system given in Eq. (12).

$$\mathrm{COP}_{ref} = \frac{\dot{Q}_{eva}^{(n)}}{\dot{W}_{com\&con}^{(n)}} = \frac{\dot{Q}_{con}^{(n)} - \dot{W}_{com\&con}^{(n)}}{\dot{W}_{com\&con}^{(n)}} \tag{12}$$

A constant COP of 3.0 is estimated for the refrigeration system using R404A by the product selection software (Emerson, ver. 1.0.65, St. Louis, USA) provided by the manufacturer. The entropy balance of system 3 is given in Eq. (13).

$$\sum_i \frac{2\dot{Q}_{cool,i}^{(n)}}{T_{s,i}^{(n)} + T_{s,i}^{(n-1)}} + \frac{\dot{Q}_{loss}^{(n)} - \dot{Q}_{con}^{(n)}}{T_{or}} + \dot{S}_{gen,out}^{(n)} = 0 \tag{13}$$

where $\dot{S}_{gen,out}$ is the entropy generation rate within system 3. The exergy balance of system 3 is given in Eq. (14).

$$\sum_i \dot{Q}_{cool,i}^{(n)} \left(1 - \frac{2T_0}{T_{s,i}^{(n)} + T_{s,i}^{(n-1)}}\right) + \left[\dot{Q}_{loss}^{(n)} - \dot{Q}_{con}^{(n)}\right]\left(1 - \frac{T_0}{T_{or}}\right) + \dot{W}_{ven} + \dot{W}_{com\&con}^{(n)} - \dot{E}x_{D,out}^{(n)} = 0 \tag{14}$$

where $\dot{E}x_{D,out}$ is the exergy destruction rate within system 3. The design details including heat transfer of the refrigeration system is not considered, so the entransy balance of system 3 is unnecessary.

3.4. Time-integral evaluation

The fractional unaccomplished temperature change (FUTC) of the produce is used to describe the progress of the precooling process as given in Eq. (15) [1].

$$Y_{t,i} = \frac{T_{t,i} - T_a}{T_{o,i} - T_a} \tag{15}$$

where the subscripts *o* and *t* respectively represent the start and any time of the process and the subscript *a* represents the cold air. The seven-eighths cooling time (SECT) can be then given with the FUTC of 0.125 and the longest SECT is considered as the operating time of the whole precooling process [31]. The discretized time integration of transient quantity leads to time-cumulative quantity as given in Eq. (16).

$$\Gamma = \sum_n \dot{\Gamma}^{(n)} \Delta t \tag{16}$$

where $\dot{\Gamma}$ is any of the transient quantities and Γ is the time-cumulative quantity. The time-integral evaluation parameters of the thermodynamic performances can be then defined based on the time-cumulative quantities. The heat rejection from all bins is the necessary cooling load, while the heat loss to the room space and the heat transformed from the ventilation power are the additional cooling loads. The ratios of the time-cumulative necessary and total cooling loads to the corresponding time-cumulative work input to systems 2 and 3 are respectively defined as the necessary and total cooling COPs for the two systems. It should be noted that these COPs are different from the COP of the refrigeration system defined in Eq. (12) which is set to be a constant value based on the evaporation and condensation temperatures. The ratio of the time-cumulative entropy generation to the time-cumulative entropy inflow is defined as the entropy generation ratio for systems 2 and 3 to evaluate the thermodynamic loss. In consideration of the work input, the ratio of the time-cumulative exergy destruction to the sum of time-cumulative heat exergy inflow and work input is also defined as the exergy destruction ratio for systems 2 and 3 to evaluate the thermodynamic loss. For system 2, the entransy dissipation ratio is defined as the ratio of time-cumulative entransy dissipation to the sum of time-cumulative heat and work entransy inflow to evaluate the heat transfer ability loss.

4. Results and discussion

The effects of the sampling positions of produce temperature on the thermodynamic performances, including energetic performances in terms of inevitable and total COPs, thermodynamic loss in terms of ratios of entropy generation and exergy destruction and heat transfer ability loss in terms of entransy dissipation ratio, are respectively compared and discussed at the room scale and ensemble scale for RC and FAC. The volumetric mean value of produce temperature is respectively obtained by the numerical and simplified methods as denoted by the dashed and dotted columns in the following figures. Moreover, the average volumetric mean value of produce temperature obtained by these two methods is represented by the solid column in the following figures and is used to compare the effects of different sampling positions inside a bin.

The effects of sampling positions of produce temperature on inevitable COP are shown in Fig. 4(a). Similar inevitable COP is obtained at the room scale for RC with the sampling positions at the inner and outer sides of the bin, while the temperature measurement in the center of the bin results in 28% decrease because of lower cooling rate at such positions. In contrast, similar inevitable COP is obtained at the same scale for FAC with the sampling positions at the inner side and in the center of the bin, while the temperature measurement at the outer side of the bin results in 31% increase because the inner side of the bin is subjected to higher air temperature inside the air tunnel resulting in lower cooling rate. These relationships keep similar at the ensemble scale for both of RC and FAC with the smaller differences of around 10%. In addition, the maximum deviations of below 10% caused by different methods to estimate the volumetric mean produce temperature are respectively observed with the sampling positions at the inner and outer sides of the bin at the room scale for RC and FAC. The effects of sampling positions of produce temperature on total COP given in Fig. 4(b) indicate similar effects on inevitable COP. However, as the value of total COP is higher than that of inevitable COP, such effects are a little less significant.

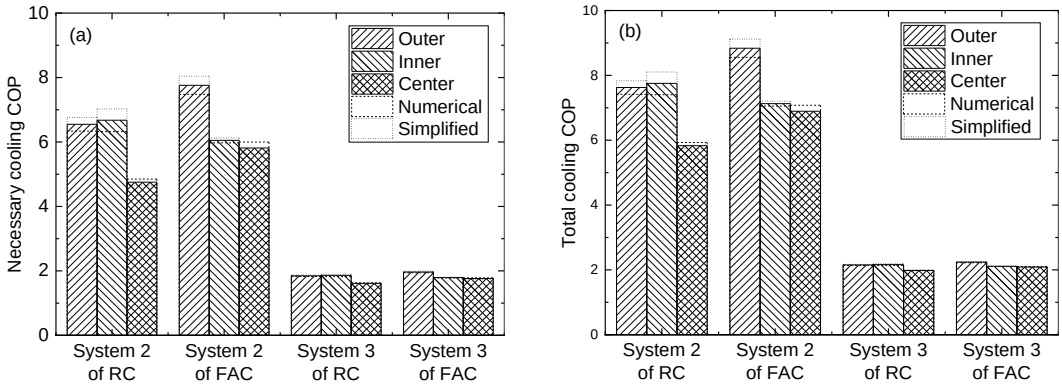

Fig. 4. Effects of sampling positions of produce temperature on energetic performances.

The effects of sampling positions of produce temperature on entropy generation ratio are shown in Fig. 5(a). Similar entropy generation ratio is respectively obtained for RC with the sampling positions at the inner and outer sides of the bin and for FAC at the inner side and in the center of the bin. The temperature measurement in the center of the bin for RC results in 32% increase of entropy generation ratio at the room scale, while 23% decrease is obtained for FAC at the same scale with the temperature measurement at the outer side of the bin. It is observed that high entropy generation ratio corresponds to low COP, so the reasons of the above effects are in consistent with that mentioned for the effects on COP. Because of higher value of entropy generation ratio at the ensemble scale, about half of the above difference of entropy generation ratio with different sampling positions of produce temperature is obtained. The deviations of entropy generation ratio caused by different methods to estimate the volumetric mean produce temperature are below 5%. The effects of sampling positions of produce temperature on exergy destruction ratio given in Fig. 5(b) are also similar with that on entropy generation ratio. However, the limited differences of exergy destruction ratio among different sampling positions of produce temperature are around or below 5% because of higher value of exergy destruction ratio.

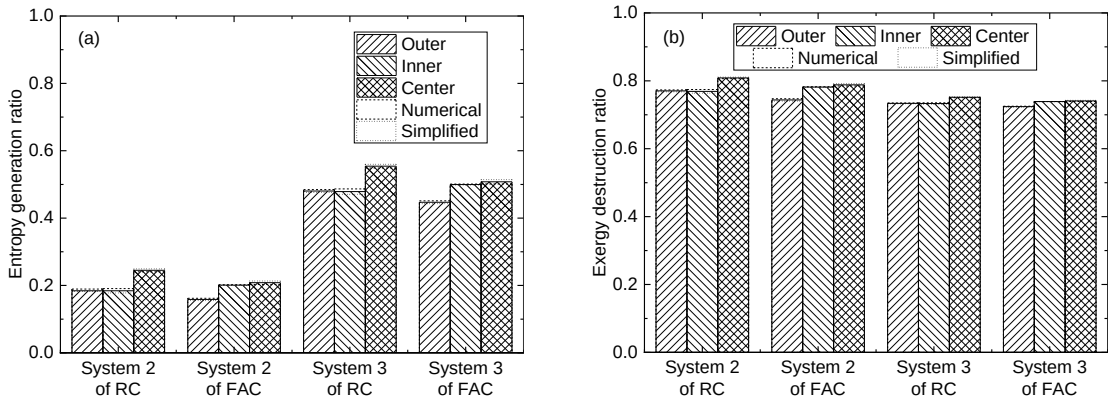

Fig. 5. Effects of sampling positions of produce temperature on thermodynamic loss.

The effects of sampling positions of produce temperature on entransy dissipation ratio are shown in Fig. 6. Different temperature measurement positions result in similar entransy dissipation ratio at the room scale for RC with limited difference of below 4%. Moreover, 6-7% deviation of entransy dissipation is obtained by different methods to estimate the volumetric mean produce temperature with the sampling positions of produce temperature at the inner and outer sides of the bin. In contrast, similar entransy dissipation ratio is obtained at the same scale for FAC with the sampling positions at the inner side and in the center of the bin, while the temperature measurement at the outer side of the bin results in 14% lower entransy dissipation ratio because of the higher cooling rate at such positions. In addition, the maximum deviation of about 7% caused by different methods to estimate the volumetric mean produce temperature is observed with the sampling positions at the outer side of the bin.

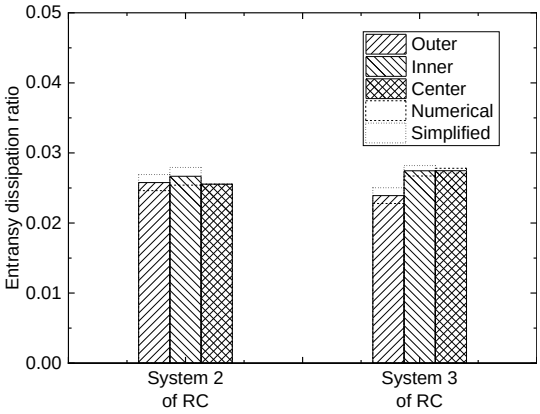

Fig. 6. Effects of sampling positions of produce temperature on heat transfer ability loss.

5. Conclusions

The comparison of thermodynamic performances of RC and FAC for postharvest apples is conducted based on the evaluation by the measured produce temperature. In consideration of the heterogenous temperature distribution within a single bin, the thermodynamic performances are evaluated with different sampling positions of produce temperature including the corners and the center of the bin. Based on the temperature measurement at the core and surface of the sampled produce individuals, the estimation of the volumetric mean produce temperature is respectively achieved by the numerical and simplified models. The main concluding remarks are as follows.

- The sampling positions of produce temperature in the center of the bin result in lower energetic performances and higher thermodynamic loss for RC than that with other temperature measurement positions, while higher energetic performances and lower thermodynamic loss for FAC are obtained with the measured produce temperature at the outer side of the bin. The differences caused by different temperature measurement positions are above 20-30% for the

COPs and entropy generation ratio at the room scale and become above 10% at the ensemble scale. The effects of different sampling positions of produce temperature are insignificant on entransy dissipation ratio for RC and exergy destruction ratio for both precooling processes with limited differences of around or below 5%, while the produce temperature measurement at the outer side of the bin leads to 14% lower entransy dissipation ratio at the room scale for FAC.

- Different methods to estimate the volumetric mean produce temperature generally result in limited effects on the thermodynamic performances. Such effects on the COPs and entransy dissipation ratio are relatively more significant with the deviations of above 5% when the produce temperature is measured at the inner and outer sides of the bin at the room scale respectively for RC and FAC.

Acknowledgments

The support of National Key Research and Development Program (2016YFD0400106) and the support from Beijing Engineering Research Center of City Heat are gratefully acknowledged.

Nomenclature

A	surface area, m^2
C	specific heat, J/(kg·K)
$\dot{Ex}$	exergy rate, W
h	specific enthalpy, J/kg
K	overall heat transfer coefficient, W/(m^2·K)
M	mass, kg
$\dot{Q}$	heat generation rate per unit mass, W/kg
$\dot{q}$	heat generation rate per unit volume, W/m^3
R	radius, m
r	radius coordinate, m
$\dot{S}$	entropy rate, W/K
T	temperature, K
t	time, s
$\dot{W}$	power, W
Y	unaccomplished temperature change

Greek symbols

Γ	time-cumulative quantity
$\dot{\Gamma}$	transient quantity
Δ	step
λ	thermal conductivity, W/(m·K)
ρ	density, kg/m^3
$\dot{\Phi}$	entransy dissipation rate, W·K

Subscripts and superscripts

a	cold air
c	core
com&con	compressor and condenser
con	condenser
cool	heat rejection from the bin

D	destruction
eva	evaporator
gen	generation
i	number of the bin
in	room scale
ir	inside the room
loss	heat loss through the room wall
m	mean
(*n*)	number of the time step
o	initial state
or	outside the room
out	ensemble scale
ref	refrigeration system
res	respiration
s	surface
t	any time of the process
ven	ventilation
0	reference state

References

[1] Brosnan T., Sun D.-W., Precooling techniques and applications for horticultural products—a review. International Journal of Refrigeration 2001;24(2):154-70.

[2] Gopala Rao C., Chapter 4: Precooling of Fruits and Vegetables by Ventilation Method. In: Gopala Rao C, editor, Engineering for Storage of Fruits and Vegetables: Academic Press. 2015. p. 49-70.

[3] Gopala Rao C., Chapter 5: Forced-Air Cooling of Fruits and Vegetables. In: Gopala Rao C, editor, Engineering for Storage of Fruits and Vegetables: Academic Press. 2015. p. 71-83.

[4] Thompson J., Mejia D., Singh R., Energy use of commercial forced-air coolers for fruit. Applied Engineering in Agriculture 2010;26(5):919-24.

[5] Mukama M., Ambaw A., Berry T.M., Opara U.L., Energy usage of forced air precooling of pomegranate fruit inside ventilated cartons. Journal of Food Engineering 2017;215:126-33.

[6] Bejan A. Entropy generation minimization: the method of thermodynamic optimization of finite-size systems and finite-time processes: CRC press, 2013.

[7] Wang J., Liu W., Liu Z., The application of exergy destruction minimization in convective heat transfer optimization. Applied Thermal Engineering 2015;88:384-90.

[8] Liu W., Liu P., Wang J.B., Zheng N.B., Liu Z.C., Exergy destruction minimization: A principle to convective heat transfer enhancement. International Journal of Heat and Mass Transfer 2018;122:11-21.

[9] Chen Q., Liang X.-G., Guo Z.-Y., Entransy theory for the optimization of heat transfer – A review and update. International Journal of Heat and Mass Transfer 2013;63:65-81.

[10] Chen X., Zhao T., Zhang M.-Q., Chen Q., Entropy and entransy in convective heat transfer optimization: A review and perspective. International Journal of Heat and Mass Transfer 2019;137:1191-220.

[11] Özilgen M., Nutrition and production related energies and exergies of foods. Renewable and Sustainable Energy Reviews 2018;96:275-95.

[12] Zisopoulos F.K., Rossier-Miranda F.J., van der Goot A.J., Boom R.M., The use of exergetic indicators in the food industry – A review. Critical Reviews in Food Science and Nutrition 2017;57(1):197-211.

[13] Ozturk H.M., Hepbasli A., Experimental performance assessment of a vacuum cooling system through exergy analysis method. Journal of Cleaner Production 2017;161:781-91.

[14] Wang G.-B., Zhang X.-R., Experimental performance comparison and trade-off among air-based precooling methods for postharvest apples by comprehensive multiscale thermodynamic analyses. International Journal of Energy Research 2019:1-21.

[15] Laguerre O., Hoang H.M., Flick D., Experimental investigation and modelling in the food cold chain: Thermal and quality evolution. Trends in Food Science & Technology 2013;29(2):87-97.

[16] Hoang H.-M., Duret S., Flick D., Laguerre O., Preliminary study of airflow and heat transfer in a cold room filled with apple pallets: Comparison between two modelling approaches and experimental results. Applied Thermal Engineering 2015;76:367-81.

[17] Zhao C.-J., Han J.-W., Yang X.-T., Qian J.-P., Fan B.-L., A review of computational fluid dynamics for forced-air cooling process. Applied Energy 2016;168:314-31.

[18] Caro-Corrales J., Cronin K., Gao X., Cregan V., Heat transfer analysis of cheese cooling incorporating uncertainty in temperature measurement locations: Application to the industrial process. Journal of Food Engineering 2010;99(2):159-65.

[19] van der Sman R.G.M., Simple model for estimating heat and mass transfer in regular-shaped foods. Journal of Food Engineering 2003;60(4):383-90.

[20] Le Bideau P., Noel H., Yassine H., Glouannec P., Experimental and numerical studies for the air cooling of fresh cauliflowers. Applied Thermal Engineering 2018;137:238-47.

[21] Jedermann R., Ruiz-Garcia L., Lang W., Spatial temperature profiling by semi-passive RFID loggers for perishable food transportation. Computers and Electronics in Agriculture 2009;65(2):145-54.

[22] Mercier S., Marcos B., Uysal I., Identification of the best temperature measurement position inside a food pallet for the prediction of its temperature distribution. International Journal of Refrigeration 2017;76:147-59.

[23] Mercier S., Uysal I., Neural network models for predicting perishable food temperatures along the supply chain. Biosystems Engineering 2018;171:91-100.

[24] Laguerre O., Duret S., Hoang H., Guillier L., Flick D., Simplified heat transfer modeling in a cold room filled with food products. Journal of Food Engineering 2015;149:78-86.

[25] Duret S., Hoang H.-M., Flick D., Laguerre O., Experimental characterization of airflow, heat and mass transfer in a cold room filled with food products. International Journal of Refrigeration 2014;46:17-25.

[26] Mercier S., Brecht J.K., Uysal I., Commercial forced-air precooling of strawberries: A temperature distribution and correlation study. Journal of Food Engineering 2019;242:47-54.

[27] Becker B.R., Misra A., Fricke B.A., Bulk refrigeration of fruits and vegetables Part I: theoretical considerations of heat and mass transfer. HVAC&R Research 1996;2(2):122-34.

[28] Lisowa H., Wujec M., Lis T., Influence of temperature and variety on the thermal properties of apples. International agrophysics 2002;16(1):43-52.

[29] ASHRAE. ASHRAE Handbook of Refrigeration: Systems and Applications. Atlanta: The American Society of Heating, Refrigerating and Air-Conditioning Engineers; 2010.

[30] Gruyters W., Verboven P., Delele M., Gwanpua S.G., Schenk A., Nicolaï B., A numerical evaluation of adaptive on-off cooling strategies for energy savings during long-term storage of apples. International Journal of Refrigeration 2018;85:431-40.

[31] Defraeye T., Cronje P., Berry T., Opara U.L., East A., Hertog M., et al., Towards integrated performance evaluation of future packaging for fresh produce in the cold chain. Trends in Food Science Technology 2015;44(2):201-25.